IOP Conf. Series: Materials Science and Engineering **148** (2016) 012039 doi:10.1088/1757-899X/148/1/012039

Analysis of motion of the body of a motor car hit on its side by another passenger car

M Gidlewski[1,3] and L Prochowski[2,1]

[1]Automotive Industry Institute, 03-301 Warszawa, ul. Jagiellońska 55, Poland
[2]Military University of Technology, 00-908 Warszawa, ul. Gen. S. Kaliskiego 2, Poland
[3]University of Technology and Humanities, 26-600 Radom, ul. Malczewskiego 29, Poland

E-mail: m.gidlewski@pimot.eu

Abstract. Based on an analysis of the course of a few experimental crash tests, a physical model and afterwards a mathematical model were prepared to describe the motion of bodies of the vehicles involved during the phase of impact. The motion was analysed in a global coordinate system attached to the road surface. Local coordinate systems were also adopted with their origins being placed at the centres of mass of the vehicles. Equations of motion of the model were derived. The calculation results enabled defining the influence of the location of the point of impact against the vehicle side on e.g. the following:

– time history of the impact force exerted by the impacting car (A) on the impacted car (B) as well as characteristic values of this force and of the impulse of the impact force;
– time histories showing changes in the velocity of the centre of vehicle mass and in the angle of deviation of the velocity vector from the direction of motion of the impacted vehicle before the collision;
– trajectory of the centre of mass and angle of rotation of the body of the impacted vehicle.

The calculations were focused on the initial period of motion of the body of the impacted vehicle, up to the instant of 200 ms from the start of the collision process. After this time, the vehicles separate from each other and move independently. The results obtained from the calculations covering this initial period make it possible to determine the starting-point values of the parameters to be taken for further calculations of the free post-impact motion of the cars.

1. Introduction

Right-angle collisions of motor vehicles amount to more than 25 % of road accidents in Poland. Knowledge of the course of accidents of this kind and, first of all, exploration of the course of the dynamic interactions that take place during the right-angle collision of two motor vehicles will enable further improvement of traffic incident modelling and reconstruction methods. The identification of the dynamic interactions between the vehicles in the culminating phase of the collision process will also make it possible to analyse the processes of injury formation in vehicle occupants and will provide a basis for the creation of new personal protection and safety means.

Many articles dealing with side collisions of motor vehicles have been published. Predominantly, they present analyses of the deformation of the side of a motor vehicle body and of the distribution of forces on the barrier face [2, 3] during a right-angle and oblique impact [7]. The results of such research works are oriented at improving the vehicle occupant protection system and designing a Mobile Deformable Barrier (MDB) [5, 6, 9]. In publication [1], the displacement of a motor car hit on its side has been presented, with highlighting the influence of the stiffness of the load-bearing vehicle structure on this process. Interesting are the results of an analysis of road accidents in Japan, where the occurrence

of injuries was linked with the speed and type of the vehicle hit on its side [8]. There is a definite lack of works where the issue of impact-caused interactions between vehicles involved in a right-angle collision would be addressed. An attempt to analyse this problem has been presented in [4].
The objective of this work was to determine the influence of the place of a frontal impact of a motor car against the side of another car on the course of the impact-caused interaction between the two vehicles and on the change in the velocity vector and trajectory of the body of the impacted vehicle. In this work, experimental testing and mathematical modelling were combined together. The results presented have been obtained for the time interval 0-0.2 s. This is the period after which the vehicles separate from each other and move independently in accordance with their individual kinetic energy. Based on the experimental test results having been collected, a physical model and afterwards a mathematical model were prepared to describe the motion of bodies of the vehicles involved during the phase of impact. The motion was analysed in a global coordinate system attached to the road surface. Local coordinate systems were also adopted, with their origins being located at the centres of mass of the vehicles. The local systems were used for presenting the measurement results and for deriving the equations of motion of the model.

2. Preparation and carrying out of experimental tests

Six crash tests were performed at the Automotive Industry Institute (PIMOT) in Warsaw with the use of 12 passenger cars of the same make and model. In each test, the front of car A crashed into the left side of car B (Fig. 1). The pre-impact speed of car A was about 50 km/h and it was twice as high as that of car B. The crash tests were carried out on a test yard with dry concrete surface, in good weather conditions. During the tests, the steering wheel of each car was left free and car wheels were not braked.

The relative positions of cars A and B were changed in successive crash tests. The location of the point of impact on the side of vehicle B was defined by the distance L_{AB} between the longitudinal plane of symmetry of car A and the front wheel axis of car B (see Fig. 1). The values of the characteristic parameters of successive crash tests have been specified in Table 1.

Figure 1. Examples of the relative positions of cars A and B during the crash tests

Table 1. Velocity of vehicle A at the instant of the collision

L_{AB} [m]	0.04	0.17	1.25	1.34	2.57	2.71
Velocity V_A [m/s]	13.6	13.1	15.1	12.7	14.2	14.7

The tests were carried out with the use of Honda Accord cars manufactured in 2000-2002. The cars were in good technical condition and had undamaged and non-corroded bodies, which had not been previously repaired. At the centre of mass of each car, there was a three-axial acceleration sensor, installed together with sensors measuring the angular velocity of the vehicle body in relation to the three

coordinate axes, whose directions and senses were consistent with those of the local coordinate systems attached to the cars.

3. Calculation of the impact force applied to the side of vehicle B

To analyse the processes that took place during the vehicle collision, a global coordinate system and local coordinate systems were adopted.

- A global coordinate system $O_GX_GY_GZ_G$, attached to the road. The $O_GX_GY_G$ plane of this system is situated at the road surface level and the O_GZ_G axis is pointing vertically upwards. The O_GX_G axis is parallel to the vector of pre-impact velocity of vehicle A and the O_GY_G axis is parallel to the vector of pre-impact velocity of vehicle B.
- Local levelled coordinate systems, attached to the centres of mass of vehicle A and B. The local coordinate system $O_AX_{PA}Y_{PA}Z_{PA}$ has its origin O_A situated at the centre of mass of vehicle A, the $O_AX_{PA}Y_{PA}$ plane is parallel to the road surface plane, and the O_AX_{PA} axis is parallel to the longitudinal vehicle symmetry plane. The local coordinate system $O_BX_{PB}Y_{PB}Z_{PB}$ has its origin O_B situated at the centre of mass of vehicle B, the $O_BX_{PB}Y_{PB}$ plane is parallel to the road surface plane, and the O_BX_{PB} axis is parallel to the longitudinal vehicle symmetry plane.
- Local coordinate systems, attached to the bodies of vehicles A and B. The local coordinate system $O_AX_AY_AZ_A$ has its origin O_A situated at the centre of mass of vehicle A and the O_AX_A axis is parallel to the longitudinal vehicle centre line. The local coordinate system $O_BX_BY_BZ_B$ is fixed to the body of vehicle B. The origin O_B of this system is situated at the centre of mass of vehicle B and the O_BX_B axis is parallel to the longitudinal vehicle centre line.

Before the collision, the axes of the local coordinate systems $O_AX_{PA}Y_{PA}Z_{PA}$ and $O_AX_AY_AZ_A$ are parallel to the corresponding axes of the global coordinate system and the local coordinate systems $O_BX_{PB}Y_{PB}Z_{PB}$ and $O_BX_BY_BZ_B$ are rotated in relation to the global system by an angle of 90 deg around the vertical axis. The positions of the local coordinate systems relative to the global system are defined by angles Φ_i – vehicle roll angle (angle of rotation around the O_ix_i axis), Θ_i – vehicle pitch angle (angle of rotation around the O_iy_i axis), and Ψ_i – vehicle yaw angle (angle of rotation around the O_iz_i axis). Subscript "i" indicates vehicle A or B.

The system of equations (1), which constitutes a basis for calculating the impact force acting between the vehicles, represents the state of equilibrium of the model reduced to the $O_GX_GY_G$ plane. This model with the system of forces under consideration has been shown in Fig. 2.

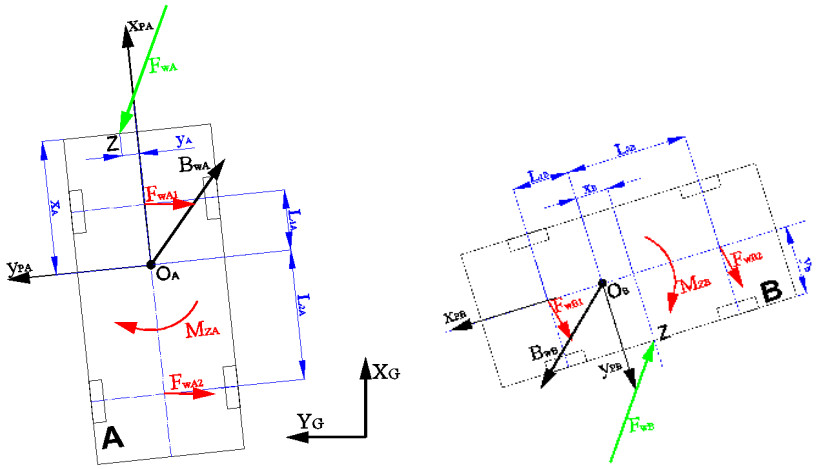

Figure 2. Coordinate systems adopted, basic dimensions used, and position of the impact force vector.

$$\begin{cases} m_A \cdot a_{xPA} = F_{nA} + F_{xA1} + F_{xA2} \\ m_A \cdot a_{yPA} = F_{sA} + F_{yA1} + F_{yA2} \\ I_A \cdot \ddot{\Psi}_A = F_{sA} \cdot x_A - F_{nA} \cdot y_A + F_{yA1} \cdot L_{1A} + F_{yA2} \cdot L_{2A} \\ m_B \cdot a_{xPB} = F_{sB} + F_{xB1} + F_{xB2} \\ m_B \cdot a_{yPB} = F_{nB} + F_{yB1} + F_{yB2} \\ I_B \cdot \ddot{\Psi}_B = F_{nB} \cdot x_B - F_{sB} \cdot y_B + F_{yB1} \cdot L_{1B} + F_{yB2} \cdot L_{2B} \\ F_{nB} = F_{nA} \cdot \cos\gamma_{AB} - F_{sA} \cdot \sin\gamma_{AB} \\ F_{sB} = F_{nA} \cdot \sin\gamma_{AB} + F_{sA} \cdot \cos\gamma_{AB} \end{cases} \quad (1)$$

where:
B_i (B_{ix}, B_{iy}) – inertial force acting on the i[th] vehicle; i = A or i = B;
M_{zi} – moment of inertia acting on the vehicle;
m_i, I_i – vehicle mass and mass moment of inertia of the vehicle relative to the vertical axis;
a_{xPi}, a_{yPi} – longitudinal and lateral components of the vector of acceleration of the centre of vehicle mass, calculated from (3);
F_{i1} (F_{xi1}, F_{yi1}) – tangent road reaction acting on the wheels of the front vehicle axle and the components of this reaction force (longitudinal and lateral, respectively);
F_{i2} (F_{xi2}, F_{yi2}) – tangent road reaction acting on the wheels of the rear vehicle axle and the components of this reaction force;
F_{wi} (F_{ni}, F_{si}) – impact force acting on the vehicle and the longitudinal and lateral components of this force;
x_i, y_i – coordinates of point Z, i.e. the point of application of the impact force, in the levelled coordinate system (Fig. 2);
γ_{AB} – angle of rotation of vehicle B relative to vehicle A around the vertical axis during the collision.

The quantities recorded during the crash tests included components of the vector of acceleration of the centre of vehicle mass (a_{xi}, a_{yi}, a_{zi}) and components of the vector of angular velocity of each vehicle (P_i, Q_i, R_i), measured in relation to the local coordinate system fixed to vehicle A or B. Example measurement results in the form of time histories of acceleration a_{yB} and angular velocity R_B have been presented in Fig. 3.

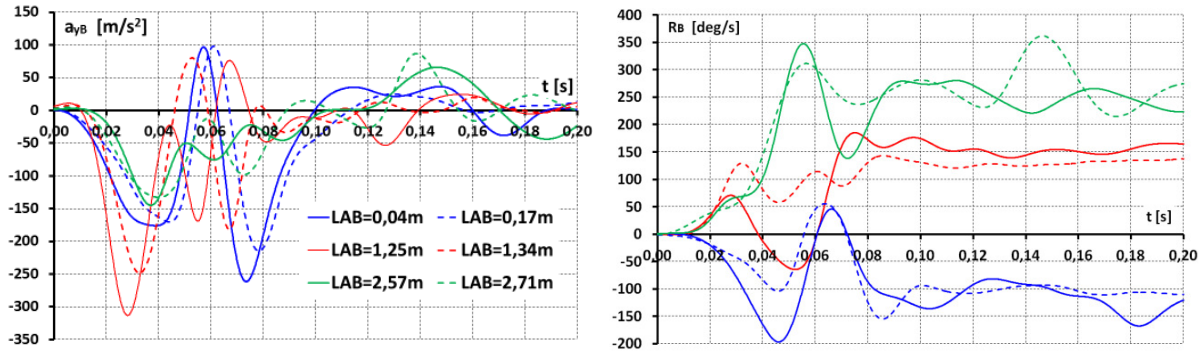

Figure 3. Lateral acceleration of the centre of mass of vehicle B (a_{yB}) and angular velocity of the body of the same vehicle relative to axis O_BZ_B (R_B) in the local coordinate system $O_BX_BY_BZ_B$ (low-pass filtered with a cut-off frequency of 50 Hz).

The values of the quantities used in equations (1), i.e. the angular accelerations of the vehicle body relative to the vertical axis and the components of the acceleration of the centre of vehicle mass, were calculated with using the results obtained from the experiment and the relations between the coordinate

systems. The kinematic calculations, the results of which were used at the analysis of the post-impact motion of the vehicles, were carried out with taking into account a transformation of the measurement results from local coordinate systems of vehicles A and B to the global coordinate system. The transformation matrices (2, 3, and 4) have been presented below:

$$\begin{bmatrix} \dot{\Phi}_i \\ \dot{\Theta}_i \\ \dot{\Psi}_i \end{bmatrix} = \begin{bmatrix} 1 & \sin\Phi_i \, tg\Theta_i & \cos\Phi_i \, tg\Theta_i \\ 0 & \cos\Phi_i & -\sin\Phi_i \\ 0 & \dfrac{\sin\Phi_i}{\cos\Theta_i} & \dfrac{\cos\Phi_i}{\cos\Theta_i} \end{bmatrix} \cdot \begin{bmatrix} P_i \\ Q_i \\ R_i \end{bmatrix} \tag{2}$$

$$\begin{bmatrix} a_{xPi} \\ a_{yPi} \\ a_{zPi} \end{bmatrix} = \begin{bmatrix} \cos\Theta_i & \sin\Theta_i \sin\Phi_i & \sin\Theta_i \cos\Phi_i \\ 0 & \cos\Phi_i & -\sin\Phi_i \\ -\sin\Theta_i & \cos\Theta_i \sin\Phi_i & \cos\Theta_i \cos\Phi_i \end{bmatrix} \begin{bmatrix} a_{xi} \\ a_{yi} \\ a_{zi} \end{bmatrix} \tag{3}$$

To determine the velocities and coordinates of the centre of mass of vehicle B in the global coordinate system, the following relation was used:

$$\begin{bmatrix} \ddot{X}_{GB} \\ \ddot{Y}_{GB} \\ \ddot{Z}_{GB} \end{bmatrix} = \begin{bmatrix} \cos(\frac{\pi}{2}+\Psi_B) & -\sin(\frac{\pi}{2}+\Psi_B) & 0 \\ \sin(\frac{\pi}{2}+\Psi_B) & \cos(\frac{\pi}{2}+\Psi_B) & 0 \\ 0 & 0 & 1 \end{bmatrix} \begin{bmatrix} a_{xPB} \\ a_{yPB} \\ a_{zPB} \end{bmatrix} \tag{4}$$

4. Results of the calculation of the impact force applied to vehicle B

Results of the calculation of the impact force F_{wB} applied to car B and its normal component F_{nBXG} in the global coordinate system have been shown in Fig. 4.

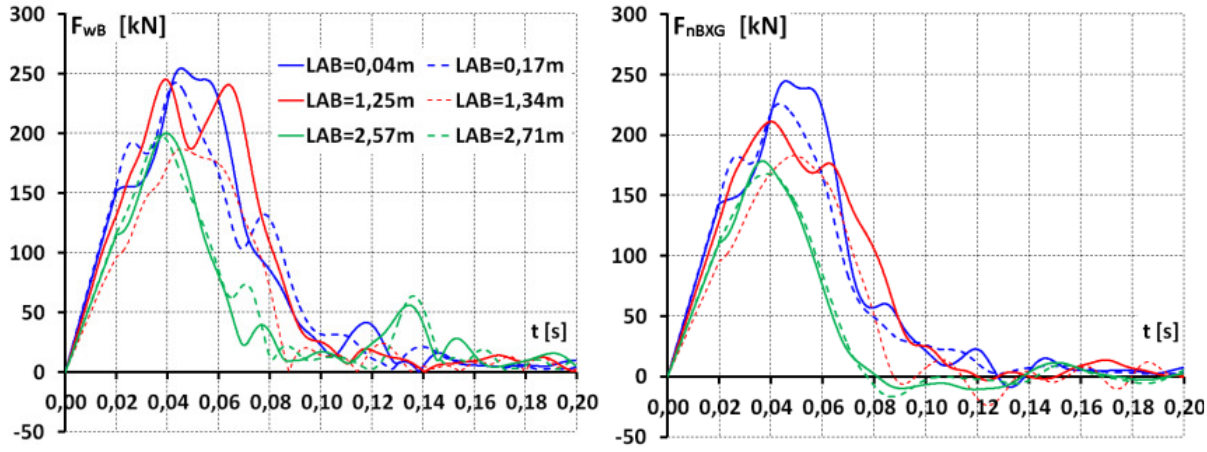

Figure 4. Time histories of the impact force F_{wB} applied to car B and of its normal component F_{nBXG} in the global coordinate system for different L_{AB} values.

The impact force vs. time curves having been determined were used for the calculations of several characteristic values, i.e.:

- extreme values of the impact force, calculated for time intervals of 3 ms, 5 ms, and 10 ms;
- impulse of the impact force, lasting during the period from 0.03 s to 0.06 s.

The time history of the impact force has the nature of a quick-changing process. Therefore, the extreme (instantaneous) values of this force do not have a decisive influence on the post-impact motion of vehicle B; they are strongly dependent upon the low-pass filter used. In this consideration, the maximum values obtained after averaging the function F_{nBXG} (t) over time intervals of 3 ms, 5 ms, and 10 ms have been given in Table 2. Such a method of load presentation links the maximum values of the impact force with the time of duration of the resulting load. The load duration time is of decisive importance for the assessment of the effects of a side impact. Table 3 shows values of the impulse of the impact force and average values of the impact force, calculated for the time interval in which the highest values of the force F_{nBXG} were recorded.

Table 2. Extreme values of the impact force F_{nBXG} [kN], calculated over time intervals of 3 ms, 5 ms, and 10 ms, based on the time histories presented in Fig. 4

L_{AB} [m]	$\Delta t = 0.003$ s	$\Delta t = 0.005$ s	$\Delta t = 0.010$ s
0.04	244	243	241
0.17	225	225	222
1.25	211	210	207
1.34	183	182	181
2.57	178	177	174
2.71	168	167	166

Table 3. Characteristic values describing the force input applied to vehicle B (Values determined on the grounds of the time history of the normal force F_{nBXG} (t))

L_{AB} [m]	Impulse of the impact force, for the period from 0.03 s to 0.06 s [Ns]	Average value of the impact force, for the period from 0.03 s to 0.06 s [kN]
0.04	6549	218
0.17	6021	201
1.25	5718	191
1.34	5047	168
2.57	4361	145
2.71	4363	145

5. Vehicle motion caused by the impact force

Below are shown the primary effects caused by the impact force, i.e.:

- time histories of the velocity of the centre of mass of vehicle B and of the angle of deflection of the velocity vector from its pre-impact direction (Fig. 5);
- trajectories of the centre of mass of vehicle B and changes in the vehicle body yaw angle Ψ_B, i.e. the angle of rotation of the vehicle body around the vertical axis (Fig. 6).

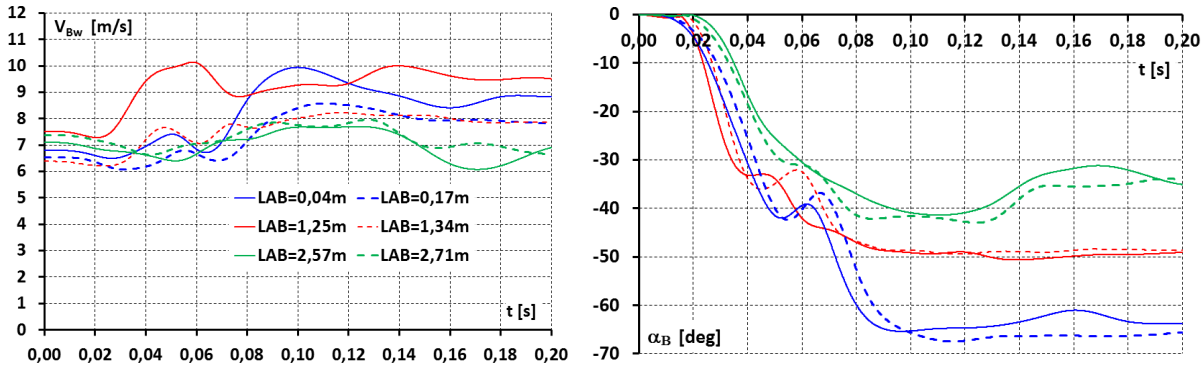

Figure 5. Velocity of the centre of mass of vehicle B and angle of deflection of the velocity vector from its pre-impact direction

The curves presented in Fig. 6 make it possible to determine the position of vehicle B on the road during the collision and at the instant of beginning of the free vehicle motion. The points marked with "×" in the graphs show the position of the centre of vehicle mass and the angle of vehicle body rotation around the vertical axis at the instant of beginning of the free vehicle motion.

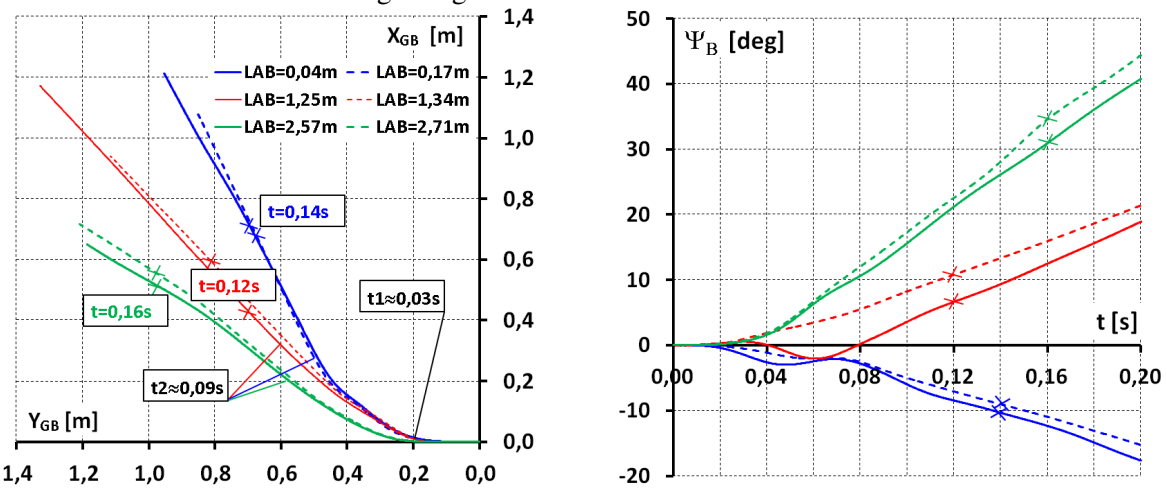

Figure 6. Trajectories of the centre of mass and changes in the body yaw angle of vehicle B

6. Vehicle body tilt versus reactions on wheels

The side impact force is balanced by the force of inertia of the impacted vehicle and the tangential reactions developing at the contact between the vehicle wheels and the road surface. Of particular interest are the lateral tangential reactions. The course of changes in their values strongly depends on the roll angle Φ_B resulting from the side impact. Fig. 7 shows the lateral tilt (roll) of the body of vehicle B at several instants in one of the crash tests (L_{AB} = 1.34 m). A time history of the roll angle Φ_B has been presented in Fig. 8, where the curves plotted have been based on measurement results obtained from six crash tests.

Noteworthy are the very high values of the vehicle body roll angle, observed not only in the contact phase of the collision process but also after the vehicle separation. A vehicle body roll angle of about 7-8 deg causes the wheel suspension on one of the vehicle sides to be fully compressed. Since the roll angle values are observed to exceed this limit, they show that the vehicle body not only tilts by rotating around the longitudinal axis O_BX_B but also rotates around an instantaneous axis going through the centres of the areas of contact between the wheels and the road on one of the vehicle sides (left or right), as it can be seen in Fig. 7. In the case illustrated there, such a rotation caused the right wheels of vehicle B to be lifted off the road surface.

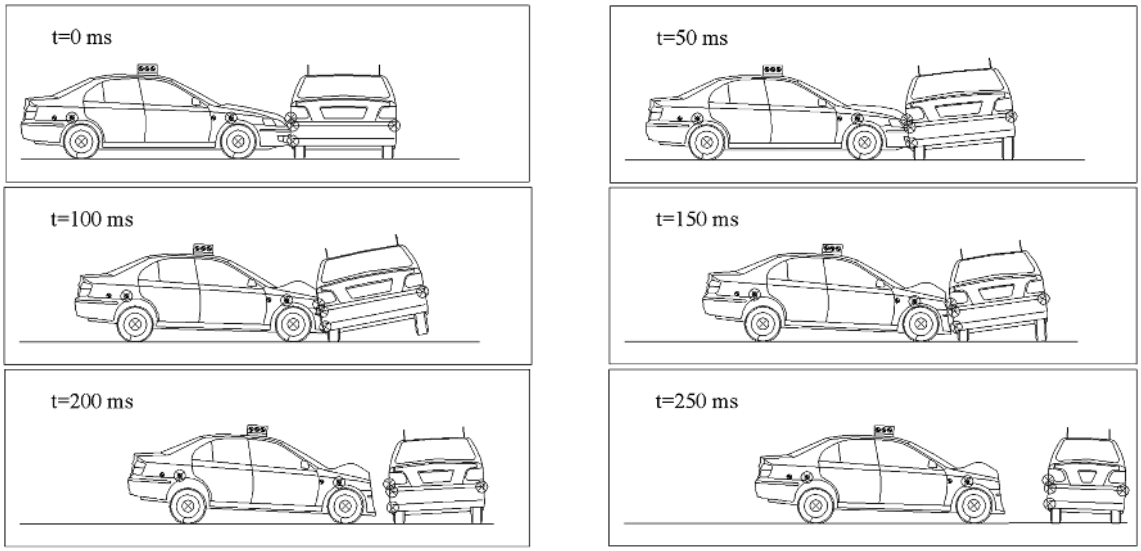

Figure 7. Lateral tilt of vehicle B caused by a side impact

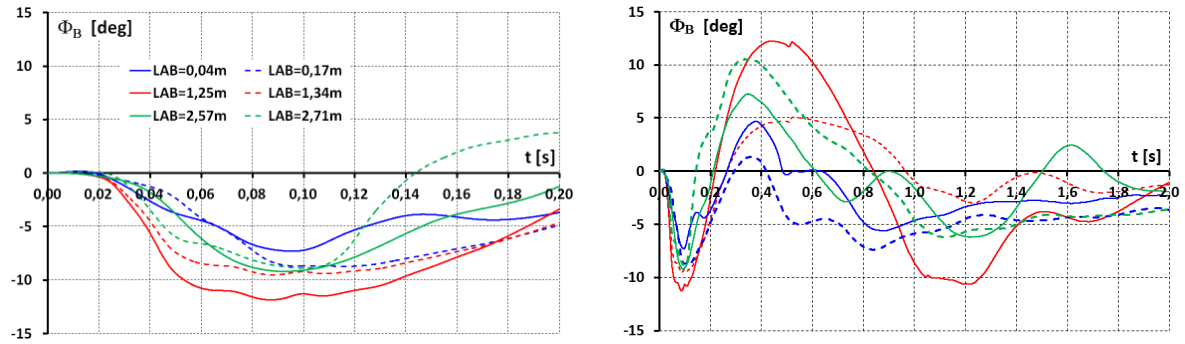

a) Roll angle $\boldsymbol{\Phi_B}$ (t = 0-0.2 s) b) Roll angle $\boldsymbol{\Phi_B}$ (t = 0-2 s)

Figure 8. Time histories of the vehicle B body angle of rotation around axis O_GX_G of the global coordinate system

Fig. 9 shows time histories of the lateral tangential road reactions on the wheels of the front and rear axle of vehicle B. The very high values of the lateral road reactions at the contact with the wheels of vehicle B were caused by very high values of the vehicle body roll angle during the collision.

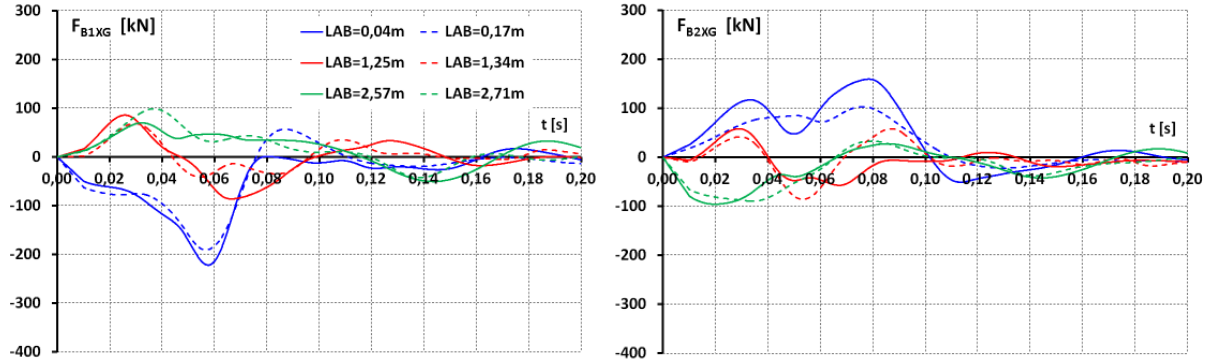

Figure 9. Lateral tangential road reactions F_{B1XG} and F_{B2XG} exerted on the wheels of the front and rear axle of vehicle B, respectively, in the global coordinate system

7. Recapitulation and conclusions

The test results obtained and the test result analysis carried out show, first of all, characteristics of the process of generating dynamic effects on the body of a motor car being struck on its side. The impact-caused interaction between vehicles (impact force) chiefly depends on the vehicle deformation process, development of the inertial resistance force exerted by the impacted vehicle, and development of the tangential reactions in the area of contact between the vehicle wheels and the road. Each of these factors has a complex influence on the time history of the impact force.

The calculations carried out were focused on the initial period of vehicle motion, up to the instant of 0.2 s from the start of the collision process. After this time, the vehicles separate from each other and move independently. The results obtained from the calculations covering this initial period make it possible to determine the starting-point values of the parameters to be taken for further calculations of the free post-impact motion of the cars.

The measurement and calculation results enabled defining the influence of the location of the point of impact against the vehicle side on e.g. the following:

- time history of the impact force exerted by car A on car B as well as characteristic values of this force and of the impulse of the impact force;
- time histories of the angular velocity of the vehicle body, translational velocity of the centre of vehicle mass, and angle of deviation of the vector of this velocity from the initial direction of motion of car B;
- trajectory of the centre of mass and time history of the angle of rotation of the body of car B, i.e. changes in the position of car B on the road.

An analysis of the measurement and calculation results provided grounds for formulating the following conclusions:

1. The values that characterize the impact force and the impulse of the impact force (Tables 2 and 3) decrease with increasing distance L_{AB} between the place of impact and the front axle of car B.
2. When car B is hit on a place close to its front axle, its pre-impact speed is raised by about 30 % (Fig. 5) and the direction of its velocity vector is changed by about 65 deg; when the point of impact is situated close to the rear axle of car B, the pre-impact speed of the impacted vehicle is decreased by about 7 % and the direction of the vehicle velocity vector is changed by about 35 deg. The changes in the magnitude and direction of the vector of velocity of the centre of mass of a car hit on its side decrease with increasing distance L_{AB}.
3. At the end of the phase of contact between the vehicles, the lateral and longitudinal displacement of the centre of mass of car B does not exceed 1 m (Fig. 6) for all the values of distance L_{AB}. At this instant, the angle of rotation of the vehicle body around the vertical axis is within a range from −10 deg to 30 deg, increasing with a growth in distance L_{AB}. After the separation of the vehicles, the direction of motion of the centre of mass of car B is approximately rectilinear and deflected from the direction of the pre-impact motion by an angle, the value of which decreases with increasing distance L_{AB}.
4. The lateral reactions at the contact between the wheels of vehicle B and the road reach very high values, of up to 80 % of the value of the impact force.

The tests reported herein were carried out and their results were analysed within an authors' own research project No. N N509 559440.

References

[1] Bumjin K, Hyunwoo K, Dongho P 2013 Research on the AE-MDB CAE analysis for the improved Euro NCAP side impact test procedure. *Proceedings of the 23rd International Technical Conference on the Enhanced Safety of Vehicles (ESV)*

[2] Digges K, Eigen A 2001 Measurements of vehicle compatibility in front-to-side crashes. *Proceedings of the 2001 International IRCOBI Conference on the Biomechanics of Impact, Isle of Man*

[3] Digges K and Eigen A 2001 Measurements of stiffness and geometric compatibility in front-to-side crashes.
[4] Gidlewski M, Prochowski L and Zielonka K 2015 Analysis of the Influence of Motor Cars' Relative Positions During A Right-Angle Crash on the Dynamic Loads Acting on Car Occupants and the Resulting Injuries. *Paper Number 15-0107. Proceedings of the 24th International Technical Conference on the Enhanced Safety of Vehicles (ESV)*
[5] Malak A, Poisson P and Touratier D 2013 Evaluation of the AFL advanced European mobile deformable barrier for side impact versus the ECE-R95 in dynamic load cell wall test. *Proceedings of the 23rd International Technical Conference on the Enhanced Safety of Vehicles (ESV)*
[6] Roberts A K and van Ratingen M R 2003 Progress on the development of the advanced European mobile deformable barrier face (AE-MDB). *Proceedings of the 18th International Technical Conference on the Enhanced Safety of Vehicles (ESV)*
[7] Welsh K J and Struble D E 1999 Crush energy and structural characterization. *SAE Technical Paper* No. 1999-01-0099
[8] Yonezawa H, Harigae T, Ezaka Y 2001 Japanese research activity on future side impact test procedures. *Proceedings of the 17th International Technical Conference on the Enhanced Safety of Vehicles (ESV)*
[9] Yonezawa H, Minda H, Harigae T, Sakurai M, Nishimoto T 2003 Investigation of new side impact test procedures in Japan. *Proceedings of the 18th International Technical Conference on the Enhanced Safety of Vehicles (ESV)*